Space group and crystal structure of the Perovskite CaTiO₃ from 296 to 1720 K

Roushown Ali[1], Masatomo Yashima[*]

Department of Materials Science and Engineering, Interdisciplinary Graduate School of Science and Engineering, Tokyo Institute of Technology, 4259 Nagatsuta-cho, Midori-ku, Yokohama, 226-8502, Japan

Abstract

The structural phase transitions of the calcium titanate perovskite $CaTiO_3$ were investigated by the Rietveld analysis of high-temperature neutron and X-ray powder diffraction data in the temperature range of 296–1720 K. The present work demonstrates that the compound exhibits two reversible phase transitions of orthorhombic *Pbnm*-tetragonal *I4/mcm* and of *I4/mcm*-cubic *Pm$\bar{3}$m* at 1498 ± 25 K and 1634 ± 13 K, respectively. No evidence of *Cmcm* phase is observed between the *Pbnm* and *I4/mcm* structures. The lattice parameters discontinuously change at the *Pbnm*–*I4/mcm* transition point, while a continuous change is observed for the *I4/mcm* − *Pm$\bar{3}$m* transformation. These results indicate that the *Pbnm*–*I4/mcm* transition is of first order and that the *I4/mcm* − *Pm$\bar{3}$m* transformation is of either second or higher order.
© 2005 Elsevier Inc. All rights reserved.

Keywords: Crystal structure; Rietveld method; Phase transition; In situ measurements

1. Introduction

Perovskite-structured compounds are promising materials in current science and technology [1], and are of fundamental importance in solid-state science and geoscience [2]. The mineral perovskite $CaTiO_3$ is the parent compound of the perovskite-structured family. It is widely used in electronic ceramic materials and in immobilizing high-level radioactive waste [3–5]. The structural phase transition of $CaTiO_3$ has been studied extensively [6–18] and reported to undergo structural changes from orthorhombic *Pbnm* to cubic *Pm$\bar{3}$m* symmetry as summarized in Table 1. Vogt and Schmahl [12] reported a direct phase transition from the *Pbnm* to *Pm$\bar{3}$m* phase and observed no intermediate phase between them. On the contrary, some research groups [8–10] reported one intermediate phase between the *Pbnm* and *Pm$\bar{3}$m* forms. Guyot et al. [11] and Kennedy et al. [13] suggested two intermediate phases including a *Cmcm* form between the *Pbnm* and *Pm$\bar{3}$m* forms. However, the existence of the *Cmcm* phase has not been established yet. Therefore, the number of existing phases in the $CaTiO_3$ is an unresolved issue and it differs from 2 to 4, depending on the literature (Table 1).

The present work has been undertaken to examine the structural phase transitions of $CaTiO_3$. In particular we focus on the possibility of the *Cmcm* phase between the *Pbnm* and tetragonal *I4/mcm* structures by using not only neutron but also X-ray powder diffraction data. With the help of higher angular resolution of the X-ray method, the present work reveals no possibility of the *Cmcm* phase. The crystal structures of all existing phases are refined by the Rietveld analyses of neutron powder diffraction data with the help of the relatively large scattering length of oxygen in neutron diffraction.

*Corresponding author. Fax: +81 45 924 5630.

E-mail address: yashima@materia.titech.ac.jp (M. Yashima).

[1] Present address: Department of Chemistry, University of Rajshahi, Rajshahi-6205, Bangladesh.

Table 1
Existing phases of CaTiO$_3$ in the literature and in the present work

Reference and method	Space groups and temperature range of existing phases			
Kay and Bailey (1957)	Orthorhombic (*Pcmn*)	Not measured		
In situ XRPD* [6]	$T \leq 1173K$	$T > 1173$		
Liu and Liebermann (1993)	Orthorhombic *(Pbnm)*	Not measured		
In situ XRPD* [7]	$T \leq 1373K$	$T > 1373K$		
Guyot et al. (1993)	*Pbnm*	Orthorhombic (*Cmcm*)**	Tetragonal or Cubic**	Cubic**
Drop calorimetry [11]	$T < 1384K$	$1384K < T < 1520K$	$1520K < T < ?$	$? < T$
Wang and Liebermann (1993)	Orthorhombic (*Pbnm*)	Tetragonal (*P4/mbm*)	Cubic	
Ex situ TEM [10]	$T < 1496K$	$1496K < T < 1585K$	$T > 1673K$	
Vogt and Schmahl (1993)	Orthorhombic (*Pbnm)*		Cubic (*Pm$\bar{3}$m*)	
In situ NPD* [12]	$T \leq 1550K$		$T \geq 1600K$	
Redfern (1996)	Orthorhombic (*Pbnm*)	Tetragonal (*I4/mcm*)	Cubic (*Pm$\bar{3}$m*)	
In situ XRPD* [8]	$T \leq 1373K$	$1423 \leq T \leq 1523K$	$T > 1523K$	
Kennedy et al. (1999)	Orthorhombic (*Pbnm*)	Orthorhombic (*Cmcm*)	Tetragonal (*I4/mcm*)	*Pm$\bar{3}$m*
In situ NPD* [13]	$T \leq 1373K$	$1398K \leq T \leq 1493K$	$1513K \leq T \leq 1573K$	$1593K \leq T \leq 1633K$
Ali and Yashima, This work	Orthorhombic (*Pbnm*)		Tetragonal (*I4/mcm*)	*Pm$\bar{3}$m*
In situ NPD and XRPD*	$T \leq 1486K$		$1523K \leq T \leq 1622K$	$T \geq 1647K$

*XRPD and NPD denote X-ray powder diffraction and neutron powder diffraction, respectively.**No crystallographic evidence but speculation from analogy with CaGeO$_3$.

2. Experimental

2.1. Sample preparation

CaTiO$_3$ sample used in this experiment was prepared by solid-state reactions. High-purity powders of CaCO$_3$ (Purity 99.99%, High-Purity-Chemical Co., Saitama, Japan) and TiO$_2$ (Purity 98.5%, Kanto-Chemical Co., Tokyo, Japan) were mixed and ground using an agate mortar as dried powders and as ethanol slurries for 3 h. The mixture was pressed into pellets under the pressure of 200 MPa and then calcined in air at 1473 K for 12 h. The pellets were crushed by an alumina mortar, and then ground by the agate mortar as dried powders and as ethanol slurries for 2 h. The powders were pressed into a rod at 200 MPa and then sintered at 1673 K for 12 h. The sintered product with a cylindrical shape of 12 mm in diameter and of 70 mm in height was used to measure the neutron powder diffraction profiles. A part of the pellet was crushed and ground into powders for X-ray powder diffraction measurements.

2.2. High-temperature neutron powder diffraction

We performed neutron powder diffraction experiments on the Kinken powder diffractometer for high-efficiency and high-resolution measurements, HERMES [19]. Incident neutrons with a fixed wavelength of 1.8196 Å were obtained by a vertically focusing (331) Ge monochromator. Diffraction data were collected at step intervals of 0.1° over a 2θ range from 20 to 152°, using 150 ^{3}He counters set at 1° intervals. We have utilized a furnace [20] with MoSi$_2$ heaters to heat the CaTiO$_3$ rod in air under atmospheric pressure at 296, 453, 661, 868, 1069, 1173, 1270, 1322, 1373, 1423, 1473, 1523, 1548, 1572, 1598, 1622, 1674, 1671 and 1720 K. There are two thermocouples in the furnace. One thermocouple near the heater was used to control the temperature and the other contacting with the rod-sample, which monitored the sample temperature. The CaTiO$_3$ rod was heated at the rate of about 10 K/min, and then the sample temperature was kept constant during each measurement, within ± 1 K above 1273 K and within ± 2 K below 1273 K.

2.3. High-temperature X-ray powder diffraction

X-ray powder diffraction data were collected at the sample temperatures of 1431, 1486 and 1598 K by an X-ray powder diffractometer with a Rotaflex X-ray generator (RINT2550V/PC, Rigaku Co. Ltd., Tokyo, Japan) under the following experimental set up: Bragg–Brentano geometry, CuKα radiation, voltage 40 kV, current 400 mA, divergence slit 0.5°, scattering slit 0.63 mm, receiving slit 0.15 mm. The measurement conditions were: Step-scanning mode with step interval

of $0.02°$ in 2θ, measuring time of 2 s, scanning range of 20–145°. The $CaTiO_3$ powder was heated using a furnace with Pt heaters attached to the goniometer of the X-ray diffractometer and the sample temperature was kept constant within ± 1.0 K during each measurement.

2.4. Rietveld analyses of neutron and X-ray diffraction data

The structural refinements of the neutron and X-ray powder diffraction data were performed by a Rietveld analysis program *RIETAN*-2000 [21]. The peak shape was assumed to be a pseudo-Voigt function with asymmetry. The background of each profile was approximated by a 12 polynomial in $2\theta^n$; where n had the value between 0 and 11. The background parameters were simultaneously refined with the lattice, peak-shape, zero-point, scale and crystal structural parameters. The following coherent scattering lengths were used for the Rietveld analysis of neutron-diffraction data: $b_{Ca} = 4.70$, $b_{Ti} = -3.37$, and $b_o = 5.803$ fm.

3. Results and discussion

3.1. Phase transitions

Neutron powder diffraction profiles of $CaTiO_3$ were measured in the temperature range of 296–1720 K. No impurity phases were detected. Each peak shifted to lower 2θ position with an increase of temperature due to the thermal expansion. The $CaTiO_3$ was identified to be the orthorhombic *Pbnm* phase with the $GdFeO_3$-type structure from 296 to 1473 K. The peak intensities of reflections such as 120, 210, 113, 122, 212, 023 and 221 of the *Pbnm* phase decreased with an increase of temperature. These *Pbnm* peaks disappeared between 1473 and 1523 K, indicating a phase transition from the *Pbnm* to an intermediate phase. The neutron-diffraction patterns show that the $CaTiO_3$ sample has an intermediate tetragonal *I4/mcm* phase from 1523 to 1622 K. Probable space groups of $R\bar{3}c$, *I4/mcm*, *Cmcm*, *P4/mbm* and *Imma* have been proposed for intermediate phases between the perovskite-type *Pbnm* and $Pm\bar{3}m$ structures [22,23]. We confirmed that the space group of the intermediate phase is neither $R\bar{3}c$, *Pbnm*, *Cmcm*, *P4/mbm*, $Pm\bar{3}m$ nor *Imma* using the neutron data of 1523–1622 K and X-ray diffraction data at 1594 K. The 211, 213, 321, 215, 323, 411, 413, 325, 431, 217, 415, 433 and 521 peak intensities of the *I4/mcm* phase decreased with an increase of temperature. These *I4/mcm* peaks disappeared between 1622 and 1647 K, indicating another phase transition from the *I4/mcm* to high-temperature cubic $Pm\bar{3}m$ phase. The $Pm\bar{3}m$ phase has an ideal cubic perovskite-type structure. In fact the

diffraction profile of the $Pm\bar{3}m$ phase exhibits only the fundamental reflections as 100, 110, 111, 200, 210 and 211. We confirmed reversible phase transitions on heating and cooling:

$$\text{Orthorhombic} \underset{Pbnm}{\overset{1498\pm25\,\text{K}}{\leftrightarrow}} \text{Tetragonal} \underset{I4/mcm}{\overset{1634\pm13\,\text{K}}{\leftrightarrow}} \text{Cubic} \underset{Pm\bar{3}m}{}$$

Within the temperature intervals of 25 and 13 K, no hysteresis was observed. This sequence of transitions is consistent with two heat anomalies observed by Guyot et al. [11]. The two heat anomalies are attributable to the *Pbnm*–*I4/mcm* and *I4/mcm*−$Pm\bar{3}m$ phase transitions, respectively, although Guyot et al. attributed them to *Pbnm*–*Cmcm* and *Cmcm*–*I4/mcm* transitions, respectively.

Guyot et al. [11] and Kennedy et al. [13] suggested another intermediate phase with *Cmcm* symmetry between the *Pbnm* and *I4/mcm* phases (Table 1). Fig. 1 shows the X-ray powder diffraction profiles at 1431 and 1486 K just below the *Pbnm*–*I4/mcm* transition point (1498 K). Splitting into the 044_{Pbnm} and 404_{Pbnm} reflection peaks is clearly observed where hkl_{Pbnm} stands for the hkl reflection of *Pbnm* phase. There is no possibility of the *Cmcm* phase, because the *Cmcm* yields only single 444 reflection. Furthermore, we obtained smaller R-factor and goodness-of-fit values ($R_{wp} = 12.3\%$, $S = 1.48$) in the Rietveld refinement of the X-ray powder diffraction data assuming the space group *Pbnm*, than those by *Cmcm* ($R_{wp} = 13.9\%$, $S = 1.68$). We also confirmed that the existing phase between 1431 and 1498 K is neither *Imma*, *P4/mbm*, *I4/mcm*, $R\bar{3}c$ nor $Pm\bar{3}m$, but the *Pbnm* phase. Thus, the *Pbnm* phase directly transforms into the intermediate *I4/mcm* structure.

3.2. Structural refinement of neutron diffraction data

The crystal structure of the neutron-diffraction data measured at 296 K was successfully refined by the $GdFeO_3$-type perovskite structure with *Pbnm* giving the following crystallographic parameters: Ca $4c$ $x,y,0.25$; Ti $4a$ $0,0.5,0$; O1 $4c$ $x,y,0.25$; and O2 $8d$ x,y,z and $a = 5.3789(2)$, $b = 5.4361(2)$, $c = 7.6388(3)$ Å (Fig. 2a and Table 2). There exists a relationship between the lattice parameters of orthorhombic phase a_o, b_o, c_o and its pseudo-cubic cell parameter $a_p : a_o \cong \sqrt{2a_p}$, $b_o \cong \sqrt{2a_p}$ and $c_o \cong 2a_p$. At the beginning of the refinement, the lattice parameters and atomic positions were refined with isotropic atomic displacement parameters where the weighted reliability factor and goodness of fit were $R_{wp} = 7.22\%$ and $S = 1.54$, respectively. Final structural refinement was performed by using anisotropic atomic displacement parameters for oxygen atoms, because significant improvements were obtained in the R-factor and goodness of fit values: $R_{wp} = 6.76\%$ and $S = 1.45$. Present lattice and
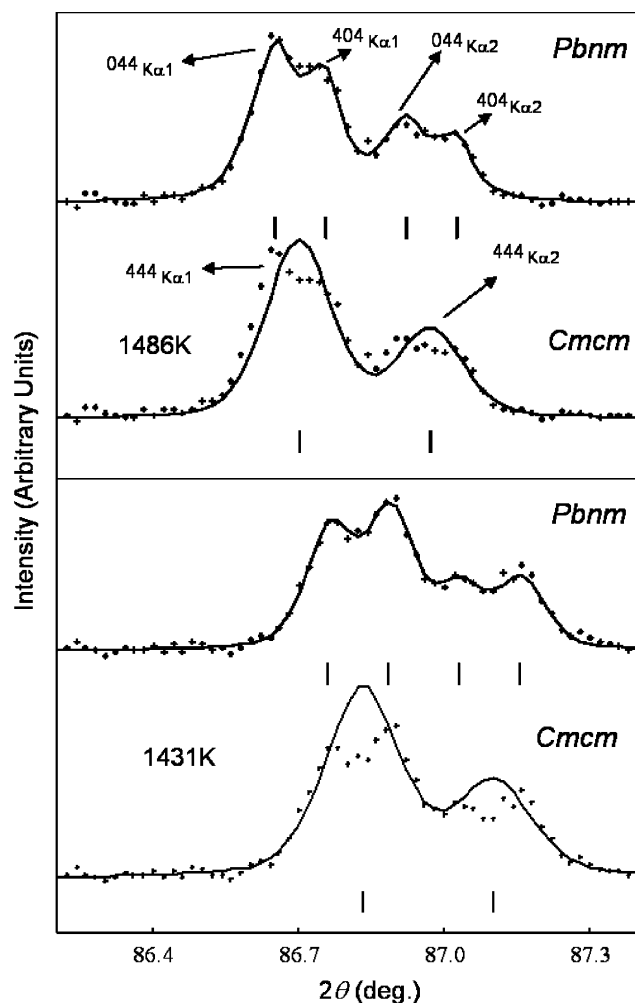
Fig. 1. A selected X-ray diffraction profiles of CaTiO$_3$ measured at 1431 and 1486 K. The cross marks are observed intensities and the solid lines are calculated profiles obtained from Rietveld analyses through *Pbnm* and *Cmcm,* and showing the comparison of the curve fit for the two space groups. Two peaks are apparent in the observed profile up to 1486 K. The *Pbnm* space group produces 044 and 404 reflections and fits well with the observed profile, whereas *Cmcm* space group produces only 444 reflection and worse fit is observed.

Fig. 2. Rietveld patterns of neutron diffraction data of CaTiO$_3$. (a) Orthorhombic *Pbnm* (296 K), (b) tetragonal *I4/mcm* (1598 K), (c) cubic *Pm$\bar{3}$m* (1720 K). The solid lines are calculated intensities and the crosses are observed intensities. The short vertical lines show the position of possible Bragg reflections. The differences between observed and calculated intensities are plotted below the profiles.

structural parameters at 296 K exhibited good agreement with those of single-crystal study reported by Sasaki et al. [24]. The lattice parameters of the present study obtained at 296 K are in agreement with those of Kennedy et al. [13] and of Liu and Liebermann [7], but differ a little from those of Redfern [8]. This difference may be ascribed to a small difference in the chemical composition.

The crystal structure of the intermediate *I4/mcm* phase was successfully refined by the Rietveld analyses of the high-temperature neutron diffraction data (Fig. 2b). The crystallographic data are tetragonal, *I4/mcm*, $Z = 4$, $a = b = 5.4984(3)$, $c = 7.7828(8)$ Å, $V = 235.29(3)$ Å^3, $D_x = 3.84$ g/cm^3, at 1598 K. The lattice parameters are characterized by the pseudo-cubic cell
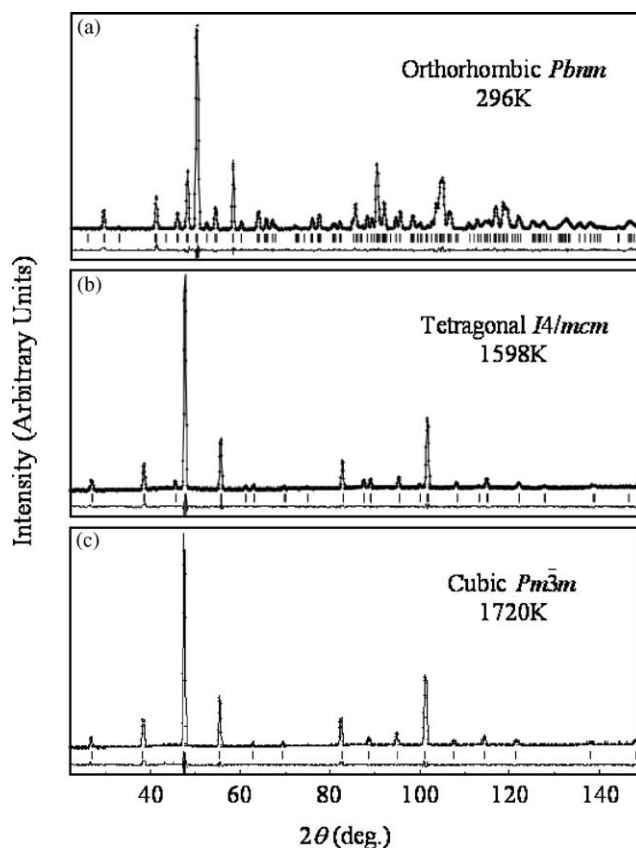
$\sqrt{2a_p} \times \sqrt{2a_p} \times 2a_p$. In the refinement of this structure, anisotropic atomic displacement parameters were considered for oxygen atoms, which makes better fit compared with that obtained with isotropic displacement parameters. The present result for the *I4/mcm* CaTiO$_3$ is consistent with that in the literature [13].

The neutron diffraction profiles above 1634 K were successfully analyzed by the ideal cubic structure with the space group *Pm$\bar{3}$m* (Fig. 2c). The crystallographic data at 1720 K of *Pm$\bar{3}$m* phase are $Z = 1$, $a = b = c = 3.8967(1)$ Å, $V = 59.167(3)$ Å^3, and $D_x = 3.82$ g/cm^3. Refinement with anisotropic atomic displacement parameters for oxygen gave a better fit in the Rietveld analysis comparing with that by isotropic parameters. On the other hand, anisotropic and isotropic thermal parameters gave similar fit for Ca and Ti atoms in the Rietveld analysis. Therefore, final refinement was performed with isotropic thermal parameters for Ca and Ti atoms and anisotropic displacement for oxygen atom (Table 2). The results are consistent with those in the literature [12,13,25].

Table 2
Lattice parameters, R-factors, positional and thermal parameters obtained from Rietveld analyses of neutron-diffraction data for three different phases of CaTiO$_3$

Temperature		296 K	1598 K	1720 K
Space group		*Pbnm*	*I4/mcm*	*Pm$\bar{3}$m*
a (Å)		5.3789(2)	5.4984(3)	3.8967(1)
b (Å)		5.4361(2)	5.4984(3)	
c (Å)		7.6388(3)	7.7828(8)	
Z		4	4	1
D$_x$ (g/cm^3)		4.04	3.84	3.82
R$_{wp}$ (%)		6.79	6.89	7.15
R$_p$		5.04	5.36	5.50
R$_F$		1.39	3.01	2.47
R$_I$		2.40	3.68	3.19
S		1.45	1.51	1.57
Ca	x	−0.0078(6)	0.0	0.0
	y	0.0357(4)	0.5	0.0
	z	0.25	0.25	0.0
	B	0.58(7)	3.80(7)	4.1(1)
Ti	x	0.0	0.0	0.5
	y	0.5	0.0	0.5
	z	0.0	0.0	0.5
	B	0.34(9)	1.9(1)	1.8(1)
O1	x	0.0736(4)	0.0	0.0
	y	0.4828(4)	0.0	0.5
	z	0.25	0.25	0.5
	B$_{eq}$	0.53	7.99	5.64
O2	x	0.7113(3)	0.2284(4)	
	y	0.2893(3)	0.7284(4)	
	z	0.0375(2)	0.0	
	B$_{eq}$	0.51	3.91	

Following the phase identification discussed above, all other neutron diffraction data measured from 296 to 1720 K were successfully refined by the Rietveld analyses. Fig. 3 shows the refined lattice parameters as a function of temperature. The lattice parameters discontinuously change at the *Pbnm*– *I4/mcm* transition point, while a continuous change is observed for the *I4/mcm*−*Pm$\bar{3}$m* transition. These results indicate that the orthorhombic-tetragonal transition is of first order and that the tetragonal–cubic transformation is of either second or higher order.

4. Conclusions

We have observed two subsequent phase transitions through neutron powder diffraction measurements in the temperature range from 296 to 1720 K. An orthorhombic *Pbnm* to tetragonal *I4/mcm* phase transition occurs at 1498 ± 25 K. Another transformation from the tetragonal *I4/mcm* to cubic *Pm$\bar{3}$m* phase occurs at 1634 ± 13 K. X-ray powder diffraction data at 1431 and 1486 K clearly showed that there is no *Cmcm* phase between the *Pbnm* and *I4/mcm* regions.
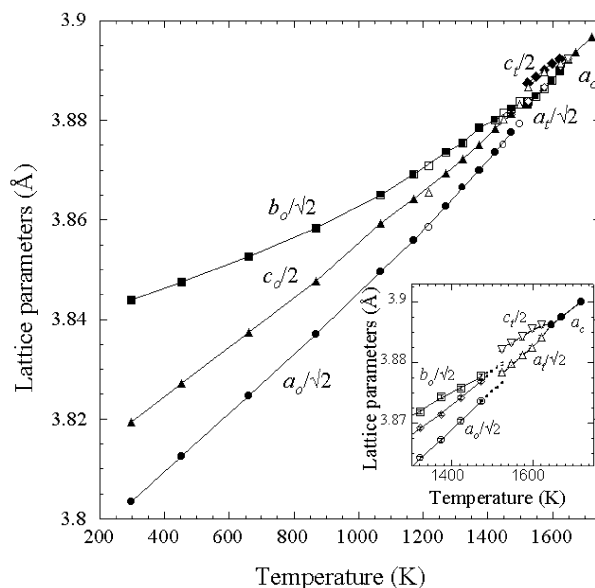

Fig. 3. Lattice parameters of *Pbnm*, *I4/mcm* and *Pm$\bar{3}$m* phases of CaTiO$_3$ as a function of temperature. Filled and open symbols indicate the data obtained on heating and cooling, respectively.

The crystal structures of the three phases were successfully refined by the Rietveld analyses of the high-temperature neutron diffraction data. The lattice parameters discontinuously change at the *Pbnm*–*I4/mcm* transition point, while a continuous change is observed for the *I4/mcm*−*Pm$\bar{3}$m* transformation. These results indicate that the *Pbnm*–*I4/mcm* transition is of first order and that the *I4/mcm*−*Pm$\bar{3}$m* transformation is of either second or higher order.

References

[1] R.E. Newnham, G.R. Ruschau, J. Am. Ceram. Soc. 74 (1991) 463–480.

[2] A.E. Ringwood, J. Geophys. Res. 67 (1962) 4005–4010.

[3] A.E. Ringwood, S.E. Kesson, K.D. Reeve, D.M. Levins, E.J. Ramm, in: W. Lutze, R.C. Ewing (Eds.), Radioactive Waste Forms for the Future, Elsevier, Amsterdam, 1988, pp. 233–266.

[4] C.J. Ball, B.D. Begg, D.J. Cookson, G.J. Thorogood, E.R. Vance, J. Solid State Chem. 139 (1998) 238–247.

[5] Y.X. Wang, W.L. Zhong, C.L. Wang, P.L. Zhang, Solid State Commun. 117 (2001) 461–464.

[6] H.F. Kay, P.C. Bailey, Acta Crystallogr. 10 (1957) 219–226.

[7] X. Liu, R.C. Liebermann, Phys. Chem. Minerals 20 (1993) 171–175.

[8] S.A.T. Redfern, J. Phys.: Condens. Matter 8 (1996) 8267–8275.

[9] T. Matsui, H. Shigematsu, Y. Arita, Y. Hanajiri, N. Nakamitsu, T. Nagasaki, J. Nucl. Mater. 247 (1997) 72–75.

[10] Y. Wang, R.C. Liebermann, Phys. Chem. Minerals 20 (1993) 147–158.

[11] F. Guyot, P. Richet, Ph. Courtial, Ph. Gillet, Phys. Chem. Minerals 20 (1993) 141–146.

[12] T. Vogt, W.W. Schmahl, Europhys. Lett. 24 (4) (1993) 281–285.

[13] B.J. Kennedy, C.J. Howard, B.C. Chakoumakos, J. Phys.: Condens. Matter. 11 (1999) 1479–1488.

[14] B.F. Naylor, O.A. Cook, J. Am. Chem. Soc. 68 (1946) 1003–1005.

[15] P. Gillet, F. Guyot, G.D. Price, B. Tournerie, A.L. Cleach, Phys. Chem. Minerals 20 (1993) 159–170.

[16] B.P. Burton, R.P. Mccormack, B.H. Toby, E.K. Goo, Ferroelectrics 194 (1997) 187–206.

[17] C.J. Howard, R. L Withers, B.J. Kennedy, J. Solid State Chem. 160 (2001) 8–12.

[18] R. Ranjan, D. Pandey, W. Schuddinck, O. Richard, P.D. Meulenaere, J.V. Landuyt, G.V. Tendeloo, J. Solid State Chem. 162 (2001) 20–28.

[19] K. Ohoyama, T. Kanouchi, K. Nemoto, M. Ohashi, T. Kajitani T., Y. Yamaguchi, Jpn. J. Appl. Phys. 37 (1998) 3319–3326.

[20] M. Yashima, J. Am. Ceram. Soc. 85 (2002) 2925–2930.

[21] F. Izumi, T. Ikeda, Mater. Sci. Forum 321–324 (2000) 198–204.

[22] K.S. Aleksandrov, Ferroelectrics 14 (1976) 801–805.

[23] K.S. Aleksandrov, Ferroelectrics 20 (1978) 61–67.

[24] S. Sasaki, C.T. Prewitt, J. Bass, Acta Crystallogr. Sect. C 43 (1987) 1668–1674.

[25] M. Yashima, M. Tanaka, J. Appl. Crystallogr. 37 (2004) 786–790.